Analytica Chimica Acta 1135 (2020) 142–149

Contents lists available at ScienceDirect

Analytica Chimica Acta

journal homepage: www.elsevier.com/locate/aca

Amino acid recognition by a fluorescent chemosensor based on cucurbit[8]uril and acridine hydrochloride

Weitao Xu [a], Huaming Feng [a], Weiwei Zhao [a], Chunhua Huang [b], Carl Redshaw [c], Zhu Tao [a], Xin Xiao [a, *]

[a] Key Laboratory of Macrocyclic and Supramolecular Chemistry of Guizhou Province, Guizhou University, Guiyang, 550025, China
[b] National Research Center for Geoanalysis, China Geological Survey, Beijing, 100037, China
[c] Department of Chemistry and Biochemistry, University of Hull, Hull, HU6 7RX, UK

HIGHLIGHTS

- A new fluorescent chemosensor comprised of Q[8] and acridine has been designed for the recognition of amino acids.
- The binding properties of Q[8] to acridine was investigated both in solid state and aqueous solution.
- A fluorescence method for the detection of five amino acids using a single system has been developed.

GRAPHICAL ABSTRACT

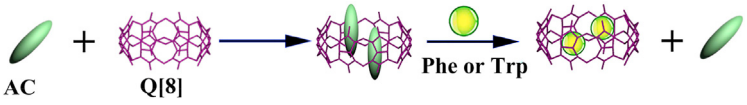

ARTICLE INFO

Article history:
Received 4 July 2020
Received in revised form
26 August 2020
Accepted 13 September 2020
Available online 25 September 2020

Keywords:
Chemosensor
cucurbit[8]uril
Recognition
"Off-on" probe
pH-responsive

ABSTRACT

A new fluorescent chemosensor comprised of cucurbit[8]uril (Q[8]) and acridine hydrochloride (AC) has been designed and utilized for the recognition of amino acids. The AC was encapsulated by the Q[8] cavity and formed a 1:2 host-guest inclusion complex both in solution (aqueous) and in the solid-state. Whilst free AC is known to be strongly fluorescent, this strong fluorescence was quenched in the inclusion complex Q [8]-AC. This non-fluorescent complex Q[8]-AC was capable of serving as a fluorescence "off-on" probe, and was able to recognize either *L*-Phe or *L*-Trp via the competitive interaction between *L*-Phe or *L*-Trp. Moreover, the pH responsive nature of the probe allowed for the detection of basic amino acids, namely *L*-Arg, *L*-His, or *L*-Lys). As a result, a fluorescence method for the detection of five amino acids using a single system has been developed.

© 2020 Elsevier B.V. All rights reserved.

* Corresponding author.
E-mail address: gyhxxiaoxin@163.com (X. Xiao).

https://doi.org/10.1016/j.aca.2020.09.028
0003-2670/© 2020 Elsevier B.V. All rights reserved.

1. Introduction

Amino acids are of huge biological significance, and are not only constituents of peptides, proteins, and alike but also play pivotal roles in the transport of materials and in biosynthesis [1,2]. Arginine (Arg) for example plays a central physiological role in a variety of transformations including cell division, gene regulation, healing of wounds and the release of hormones [3–5]. Moreover, Arg is used to treat diseases resulting from endocrine and high ammonia reactions [6,7]. Similarly, histidine (His) is critical for many enzymatic processes [8], whilst it has been reported that decreases in His levels are observed in patients suffering from lung cancer [9–13]. In the case of lysine, it is linked to the Krebs-Henseleit cycle and to polyamine synthesis [14,15], whilst high levels of lysine in the plasma and urine are indicators of congenital metabolic disorders, for example cystinuria or hyperlysinemia [16,17]. The amino acid phenylalanine (Phe) is extensively employed both in the food and pharmaceutical industries. Examples of the use of Phe include as an intermediate in the production of anti-cancer drugs, as a nutritional additive, and as an additive in food and drink [18]. Finally, from a biological perspective, tryptophan (Trp) plays an important role in human metabolism [19] and is associated with the likes of diabetes and nerve disorders [20]. The selective recognition of amino acids is thus highly desirable for a variety of medicinal reasons (see Scheme 1).

We note that a range of traditional detection methods for amino acids have previously been developed, including high-performance liquid chromatography, ion-exchange chromatography as well as gas chromatography [21–23]. However, such detection methods suffer from a number of deficiencies, namely that they are somewhat complicated, not cheap, can be awkward to use, exhibit poor selectivity, lack precision and sensitivity, and also suffer from a lack of reproducibility [24]. This has led to recent increased interest in the potential of host-guest chemistry, and a boost to progress in the area of molecular recognition [25–27]. This increased interest in aqueous host-guest chemistry has led to the availability of analyte responsive host-dye systems based on macrocycles or so-called host-dye fluorescence indicator displacement (FID) systems. Such FID systems are now attracting the interest of researchers as agreeable alternatives to the more traditional chemosensors [28,29].

Cucurbit [*n*]urils (Q [*n*]s), a family of synthetic macrocycles, are capable of binding amines over a wide affinity range (10^3 to 10^{12} M^{-1}) in aqueous solution, and for this reason have attracted interest for both molecular recognition and in molecular devices [30–39]. Over the past 10 years or so, Q[*n*]s and derivatives thereof have been shown to interact with a number of specific amino acids, peptides, and proteins [40–48]. However, given that amino acids have in common the same types of functional groups, namely carboxylic/CO_2H and amino/NH_2 groups, the manufacture of sensors capable of detecting specific amino acids with both significant sensitivity and selectivity remains a key target. Reports on the use of cucurbit [*n*]uril-based host-dye fluorescence indicator displacement systems for amino acid detection remain scant. In 2011, Quintana reported an electrochemical sensor which employed the host-guest interactions of Q[8], and was applied to the determination of tryptophan in 'real' samples displaying reasonable accuracy and precision [49]. In 2017, our group reported two fluorescent probes based on two alkyl-substituted cucurbit [6]urils and a cationic vinylpyridine containing dye. These probes were capable of recognizing lysine and methionine *versus* a number of other α-amino acids in aqueous solution [50]. More recently, Yang et al. synthesized an ambient temperature phosphorescent (RTP) cyclodextrin-Q [6]-co-wheeled [4]rotaxane, and utilized it for the highly specific sensing of Trp. It was noted that the strong green emission associated with the RTP was quenched in the presence of Trp, whereas when other physiologically relevant amino acids were added, no such quenching was evident [51].

Herein, a cucurbit [*n*]uril-based host-dye fluorescence indicator has been assembled from Q[8] and acridine hydrochloride (AC). The interaction between Q[8] and AC was studied by a number of spectroscopic methods including fluorescence, UV–vis and ^{1}H NMR spectroscopy. From the data accumulated, a 1:2 host-guest inclusion complex was identified. Interestingly, free AC is known to be strongly fluorescent, however the fluorescence was quenched for this Q[8]-AC inclusion complex. To this Q[8]-AC system, 20 natural amino acids were added; phenylalanine (Phe) and tryptophan (Trp) both resulted in a significant amplification of the green fluorescence intensity of the inclusion complex, while basic amino acids exhibited blue fluorescence. These results demonstrated the ability to detect five amino acids in a single system using a fluorescence method.

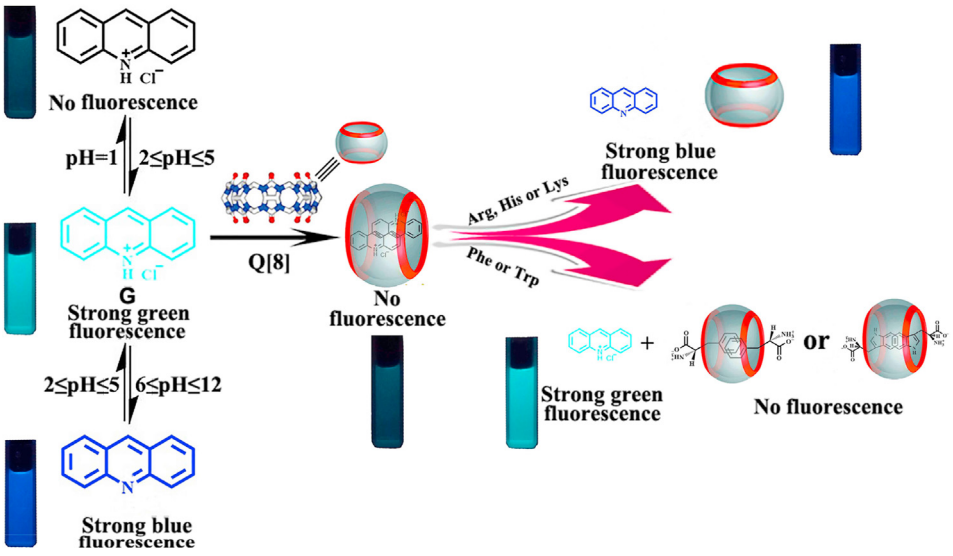

Scheme 1. A feasible process for the fluorescence indicator displacement via the host-guest interactions.

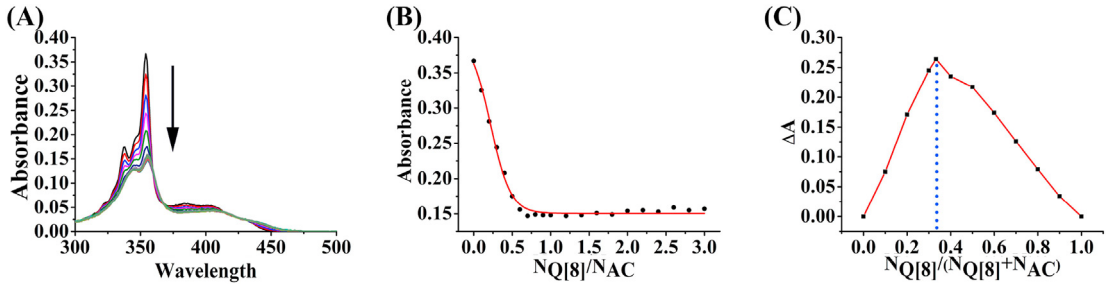

Fig. 1. (Color online) (A) Absorption of AC (2×10^{-5} mol L^{-1}) upon addition of increasing amounts (0, 0.1, 0.2·····0.9, 1.0, 1.2, 1.4·····2.6, 2.8, and 3.0 equiv) of Q[8] in aqueous HCl solution (pH = 4.0); (B) the concentration and absorbance *vs.* $N_{Q[8]}/N_{AC}$ plots in aqueous HCl solution (pH = 4.0); (C) the corresponding $\Delta A - N_{Q[8]}/(N_{Q[8]} + N_{AC})$ curves in aqueous HCl solution (pH = 4.0). (For interpretation of the references to color in this figure legend, the reader is referred to the Web version of this article.)

2. Results and discussion

2.1. Binding behavior between AC and Q[8]

The binding behavior between Q[8] and AC was initially studied by employing UV–vis absorption and fluorescence spectroscopy. The gradual addition of Q[8] results in a gradual decrease in the maximum absorbance of AC (at a fixed AC concentration of 2×10^{-5} mol L^{-1}) at 355 nm (Fig. 1A) until the ratio of the host-guest reached 0.5. This suggests a 1:2 host-guest inclusion complex is formed between the Q[8] and AC (Fig. 1B), and a continuous variation Job's plot (Fig. 1C) was also consistent with a stoichiometry of 1:2.

Given that the guest AC possesses an amino group, and that protonation/deprotonation or changes in solution pH are likely to influence the photophysical properties of AC, it is necessary to evaluate the influence of the inclusion of AC by Q[8] *versus* free AC on the p*K*a. The effect of free AC and the presence of Q[8] (0.5 equiv) *versus* pH (1–12) were tracked using UV–visible and fluorescence spectroscopy. As can be seen in Figs. S1–S2, over the pH range 1.05–4.00, AC exists in the protonated form, and the fluorescence intensity of AC increases with increasing pH. By contrast, over the pH range 5.99–11.95, the fluorescence intensity of AC decreases and this is accompanied by a blue shift on increasing pH. When comparing the absorbance-pH and fluorescence-pH curves for AC and that of the inclusion complex (Fig. S3), it was decided for this study to conduct the experiments at pH 4.0, where AC exists in the protonated form.

As mentioned above, AC (2×10^{-5} mol L^{-1}) displays a robust green fluorescence possessing a maximum emission at 478 nm in solution (aqueous) at pH 4.0 (Fig. 2A), whilst the interaction with Q[8] led to a significant weakening of the emission intensity. Also, the continued addition of Q[8] resulted in a further weakening in the emission intensity of AC until the Q[8]-AC ratio reached 1:2 (Fig. 2B), which revealed the emergence of a robust supramolecular complex. The extinguishing of fluorescence is attributed to photo-induced electron transfer from the carbonyl oxygen of Q[8] to the excited state of AC [52]. Moreover, using the Job's plot method, as shown in Fig. 2C, it was observed that the maximum peak appeared at a mole fraction of 0.33, which corresponds to a 1:2 binding stoichiometry for Q[8] to AC, and this is compatible with the results acquired from the UV–vis absorption spectra. Furthermore, the isothermal titration calorimetry experiment was carried out at 25 °C to better understand the host-guest interactions between Q[8] and AC. The experimental results afforded an association constant (K_a) value of 2.870×10^8 M^{-2}, and ΔH° and $T\Delta S^\circ$ values indicating that the interactions between the Q[8] host and AC guest appear to be driven by favorable enthalpy changes, accompanied by small negative (unfavorable) entropy changes (Fig. S4).

On using a fixed amount of AC and gradually increasing the

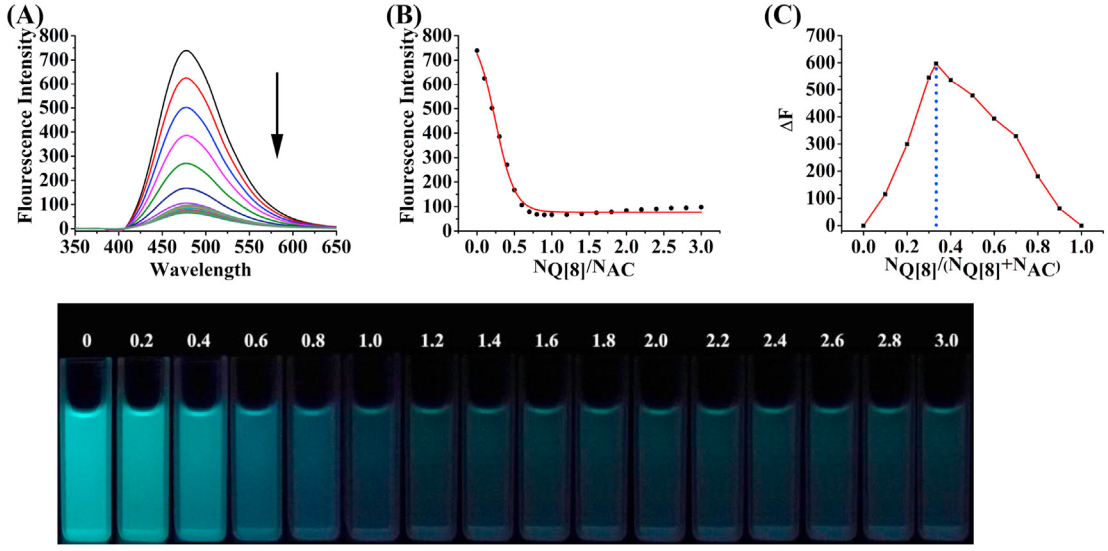

Fig. 2. (A) Fluorescence emission of AC (2×10^{-5} mol L^{-1}) following increasing amounts (0, 0.1, 0.2·····0.9, 1.0, 1.2, 1.4·····2.6, 2.8, 3.0 equiv) of Q[8] in HCl_{aq} solution (pH = 4.0); (B) the concentration and fluorescence *vs.* $N_{Q[8]}/N_{AC}$ plots in aqueous HCl solution (pH = 4.0); (C) the corresponding $\Delta F - N_{Q[8]}/(N_{Q[8]} + N_{AC})$ curves in HCl solution (pH = 4.0). (D) Photographs of AC (2×10^{-5} mol L^{-1}) upon addition of growing amounts (0, 0.2, 0.4·····2.6, 2.8, 3.0 equiv) of Q[8] under UV light (365 nm).

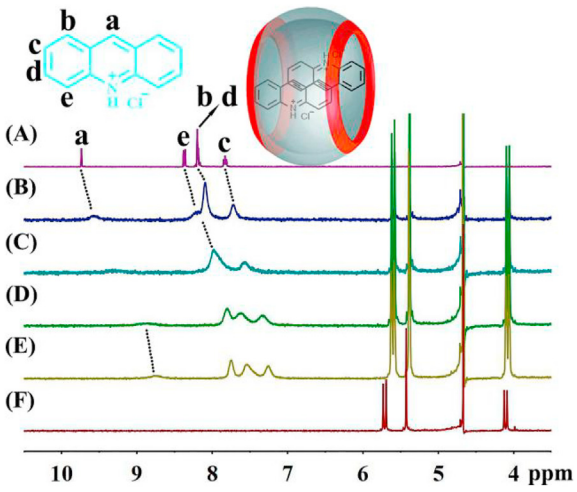

Fig. 3. Combination of AC and Q[8] at 25 °C: ^{1}H NMR spectra (400 MHz, D_2O, pD = 4.0) of AC (*ca.* 2×10^{-5} mol L^{-1}) with no Q[8] (A), with 0.17 equiv. of Q[8] (B), with 0.42 equiv. of Q[8] (C), with 0.69 equiv. of Q[8] (D), with 1.04 equiv. of Q[8] (E) and neat Q[8] (F).

amount of Q[8] present, the binding behaviour was followed by ^{1}H NMR spectroscopy (Fig. 3). Following the addition of Q[8], the proton resonances associated with the guest shifted upfield (0.99 ppm for proton H_a, 0.65 ppm for proton H_b, 0.57 ppm for proton H_c, 0.65 ppm for proton H_d, and 0.04 ppm for proton H_e), which suggested that these guest protons are included within the Q[8] cavity. These results combined with those above allowed us to predict a plausible interaction model in which the AC molecules completely enter the cavity of Q[8], see Fig. 3 (insert). The application of MALDI-TOF mass spectrometry, see Fig. S5, also provided evidence consistent with the formation of a 1:2 host-guest complex, with intense signals at 1689.022, corresponding to $[(Q[8]\text{-}2AC)\text{-}2Cl^-]^+$.

In addition, we obtained single crystals of **AC**2@Q[8]. Since the solubility of Q[8] in neutral aqueous solutions is poor, the crystallization of Q[8]-AC was performed in an aqueous solution of HCl (6.0 M) via the introduction of $[CdCl_4]^{2-}$. The structure is shown in Fig. 4, where two AC guest molecules are located within the host Q[8] cavity, forming a 1:2 stoichiometric host-guest inclusion complex, which agrees with the host-guest solution studies. Close inspection revealed that although two AC guest molecules are located in the Q[8] cavity, they assume different inclusion conformations in the structure. For one of the two inclusion complexes (Fig. 4A), $\pi\cdots\pi$ interactions between the two AC guest molecules in the Q[8] cavity could be observed, where the distance between two aromatic rings is 3.417 Å, and the angle formed between the axis of the parallel guest pair and the plane established by eight carbonyl oxygen atoms of Q[8] host is 66.20°. There also exist *C*—H···O hydrogen bond interactions arising from the hydrogen of AC and the portal carbonyl group of Q[8] (C55···O1 = 2.966 Å), as shown in the bottom right corner of Fig. 4C. For the other inclusion complex (Fig. 4B), the included guest pair interact via $\pi\cdots\pi$ interactions between the two acridine rings, which is similar to that found in the abovementioned host-guest inclusion complex. Here, the distance between two aromatic rings is 3.661 Å, while the angle between the axis of the parallel guest pair and the plane formed by the eight carbonyl oxygen atoms of Q[8] host, close to vertical, is 83.80°. Interestingly, multiple *C*—H···O and *N*—H···O hydrogen bond interactions were found between the hydrogen of the guest and the portal carbonyl group of Q[8] (C67···O14 = 3.187 Å; C68···O14 = 2.983 Å; N34···O9 = 2.922 Å, and N34···O16 = 3.043 Å) in this host-guest inclusion complex (see bottom upper left corner of Fig. 4C). The *C*—H···Cl hydrogen bonds (C3···Cl3 = 3.372 Å) between the portal carbonyl group of Q[8] and the Cl^- ions coordinated to zinc ions are present, as shown in Fig. 4C.

2.2. The response of the Q[8]-AC inclusion complex to different L-amino acids

In order to detect amino acids by fluorescence, a non-fluorescent host-guest system was designed, thereby allowing for the facile "turn-on" fluorescence sensing of amino acids. As mentioned above, this new host-guest Q[8]-AC inclusion complex is non-fluorescent and exhibits good solubility in water. In order to discover whether the Q[8]-AC inclusion complex prepared herein could be employed to identify natural amino acids, a number of fluorescence experiments were conducted using each of the natural amino acids.

Given that differing fluorescence phenomena are observed at differing pH, the detection of *L*-amino acids was initially conducted in aqueous solution at pH 4.0. As observed in Figs. 5 and 6, on addition of the 20 natural amino acids (2×10^{-4} mol L^{-1}) to the Q[8]-AC solution (2×10^{-5} mol L^{-1}), only three basic *L*-amino acids (*L*-Arg, *L*-His, or *L*-Lys) resulted in blue shift fluorescence changes (36 nm for *L*-Arg or *L*-Lys, and 8 nm for *L*-His). Moreover, when either *L*-Phe or *L*-Trp was added to the Q[8] -AC inclusion complex, a fluorescence enhancement was evident. By contrast, on adding any of the other natural amino acids under similar conditions failed to lead to well-defined fluorescent changes. Such results strongly suggest that the Q[8]-AC inclusion complex can be employed for the discrimination of Phe, Trp, and basic amino acids (*L*-Arg, *L*-His, or *L*-Lys) in aqueous solution.

A number of quantitative luminescence titration experiments were performed to further understand the recognition capability of the Q[8]-AC complex toward the above five amino acids. Firstly, different concentrations of *L*-Phe or *L*-Trp (0–3.0 × 10^{-4} mol L^{-1})

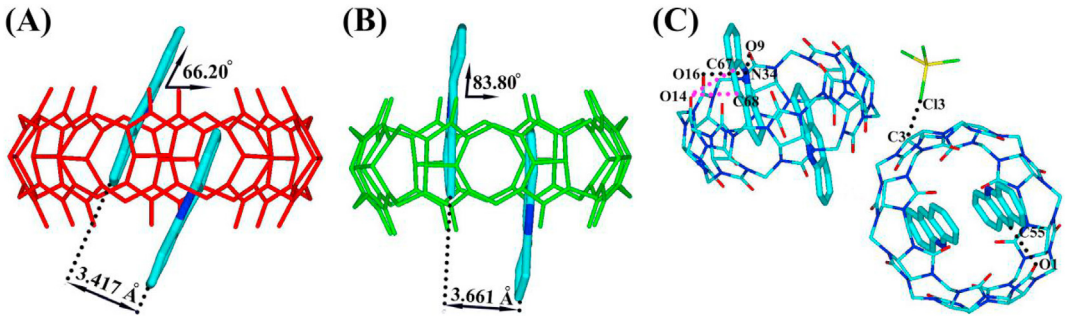

Fig. 4. The molecular structure of the homo-ternary complex **AC**2@Q[8].

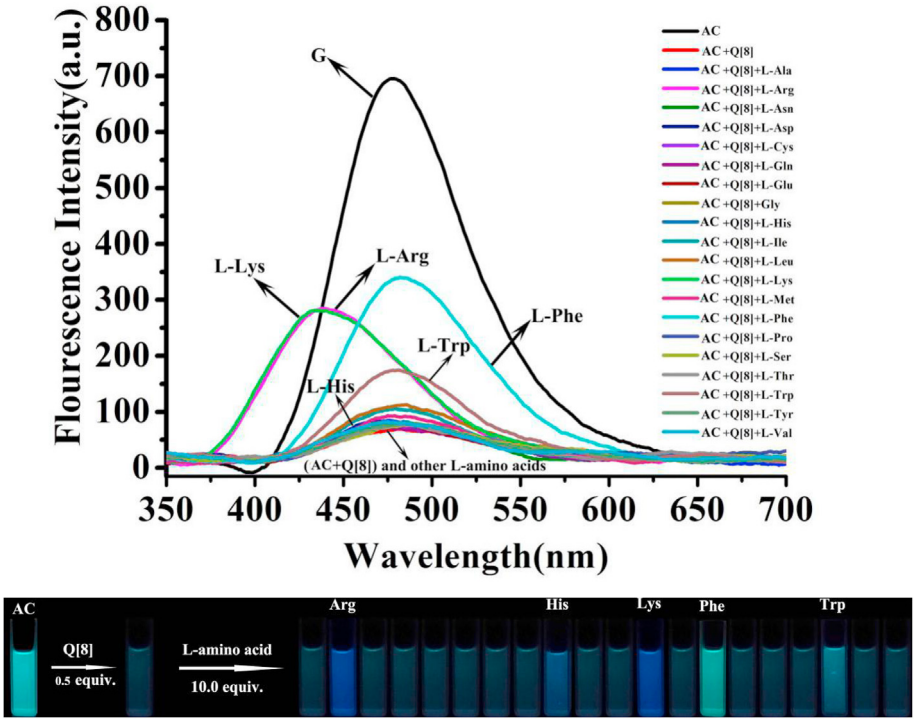

Fig. 5. (top) The effect of *L*-amino acids (10 equiv. of host-guest complex) on the fluorescence response (λmaxem = 478 nm) of AC-Q[8] (2×10^{-5} mol L^{-1}) (2:1); (bottom) photographs of AC-Q[8] systems containing 10 equiv. of host-guest complex and different *L*-amino acids under UV light (365 nm).

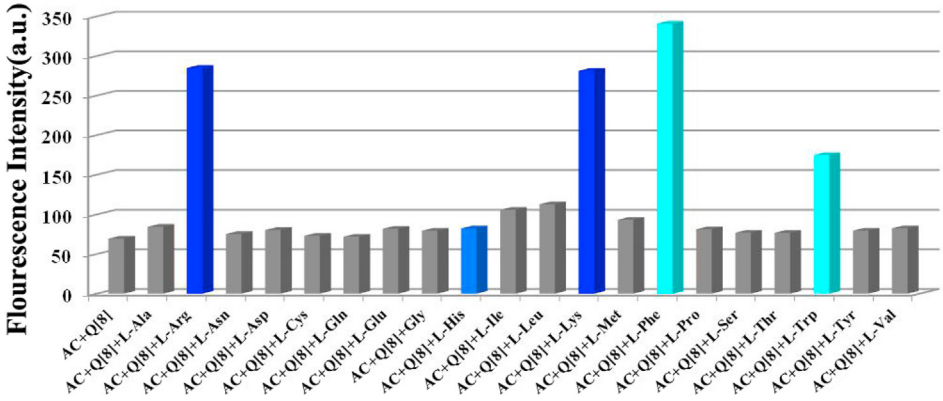

Fig. 6. The effect of *L*-amino acids (10 equiv. of host-guest complex) on the fluorescence intensity (λem = 478 nm) of AC/Q[8]](2 × 10^{-5} mol L^{-1}) (2:1).

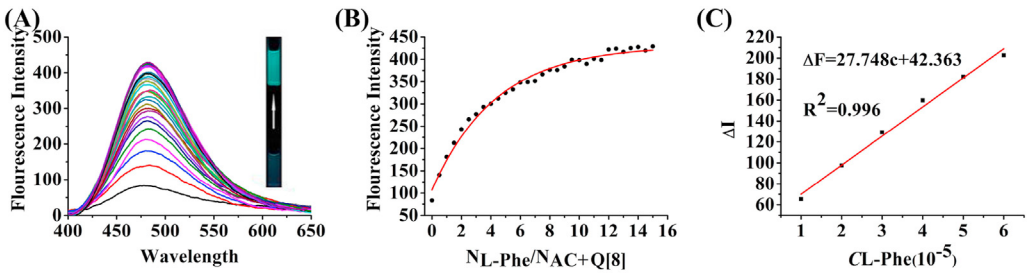

Fig. 7. (A) Titration fluorescence spectra of Q[8]-AC (2×10^{-5} mol L^{-1}) (2:1) with *L*-Phe; (B) Plots of $N_{L\text{-Phe}}/N_{AC}$ + Q[8]; (C) Non-linear fitting curves for fluorescence intensity variation of the inclusion complex for differing concentrations of *L*-Phe.

were added to an aqueous Q[8]-AC solution, and from Fig. 7 and S6 it is evident that the fluorescence intensity of the Q[8]-AC complex enhanced gradually with increasing concentration of the amino acids. The significant enhancement in fluorescence for the Q[8]-AC complex in the presence of *L*-Phe or *L*-Trp, under illumination by a 365 nm lamp, was also evident to the naked eye. The fluorescent spectra of *D*-Phe or *D*-Trp following addition to an aqueous Q[8]-AC solution were also studied (Figs. S6 and S7, ESI). In this case, it was

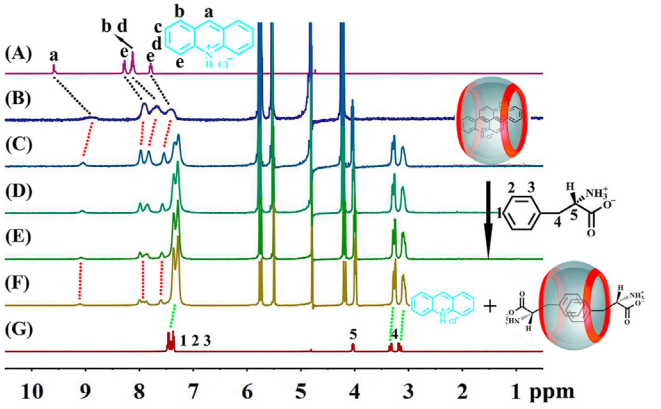

Fig. 8. Titration ^{1}H NMR spectra (D_2O, pD = 4.0) of (A) neat AC, Q[8]-AC (2:1, 2×10^{-5} mol L^{-1}) in the presence of (B) 0.00, (C) 7.15, (D) 14.33, (E) 21.26, and (F) 27.78 equiv. of *L*-Phe, and (G) neat *L*-Phe.

observed that there was no selectivity for either *L* or *D* amino acids. Over the concentration range 2.0×10^{-5} to 30.0×10^{-5} mol L^{-1}, the detection limits (DLs) for the chosen amino acids were determined to be 2.108×10^{-6} mol L^{-1} for *L*-Phe (Fig. 7C), 2.100×10^{-6} mol L^{-1} for *D*-Phe (Fig. S7C, ESI), 4.750×10^{-6} mol L^{-1} for *L*-Trp (Fig. S6C, ESI), and 3.200×10^{-5} mol L^{-1} for *D*-Trp (Fig. S8C, ESI).

Following the above strategy, three basic amino acids, namely *L*-Arg, *L*-His, or *L*-Lys were slowly added to an aqueous solution of Q[8]-AC. When between 0 and 5.0 equiv. of amino acids were added, no notable changes were evident in the fluorescence intensity of the Q[8]-AC system. However, on increasing the concentration of the basic amino acids, the fluorescence intensity gradually increased, and was accompanied by a blue shift (Figs. S9 and S11). Such observations are consistent with the gradual introduction of basic amino acids (*L*-Arg, *L*-His, or *L*-Lys) to an aqueous solution of free AC (Figs. S12–S16), and could be ascribed to pH changes as the basic amino acids were added (Tables S1 and S2).

In order to more fully understand the mechanism of recognition of the Q[8]-AC complex towards amino acids, ^{1}H NMR spectroscopy was employed using the *L*-Phe or *L*-Trp and Q[8]-AC systems in D_2O solution (pD = 4). As shown in Fig. 8, when *L*-Phe was added to the Q[8]-AC solution, the aromatic protons (H1, H2, and H3) and the methylene proton (H4) underwent a clear upfield shift, while proton H_5 exhibited a downfield shift, which indicated that the aryl ring and methylene of the *L*-Phe can be found encapsulated within the cavity of the Q[8]. The remaining part of *L*-Phe is out of the Q[8] portal, the result being an inclusion complex between Q[8] and *L*-Phe. Then, upon adding *L*-Phe to the Q[8]-AC inclusion complex in D_2O, all the proton resonances for the guest AC associated with the Q[8]-AC inclusion complex appeared to shift downfield ($H_a = 0.23$; $H_b = 0.21$; $H_c = 0.19$; $H_d = 0.21$; $H_e = 0.09$ ppm) (Fig. 8), which suggested that these protons were gradually exiting from the Q[8] cavity. Concomitantly, the protons (H_1, H_2, H_3, and H_4) of *L*-Phe shifted to lower field compared to *L*-Phe in the inclusion complex. These observations demonstrated that the *L*-Phe molecule was capable of replacing the included AC molecule in the Q[8] cavity. Based on these observations, a possible interaction model between *L*-Phe and Q[8]-AC is shown in Fig. 8 (insert). For comparison, upon addition of *D*-Phe to the Q[8]-AC inclusion complex in D_2O, the same phenomenon was observed (Fig. S21).

By using a similar approach, the mechanistic aspects of the recognition process of the Q[8]-AC complex towards *L*-Trp was also investigated in D_2O solution (pD = 4), and was monitored by ^{1}H NMR spectroscopy. As shown in Fig. S22, upon adding *L*-Trp to the Q[8]-AC inclusion complex in D_2O, the included AC molecule was

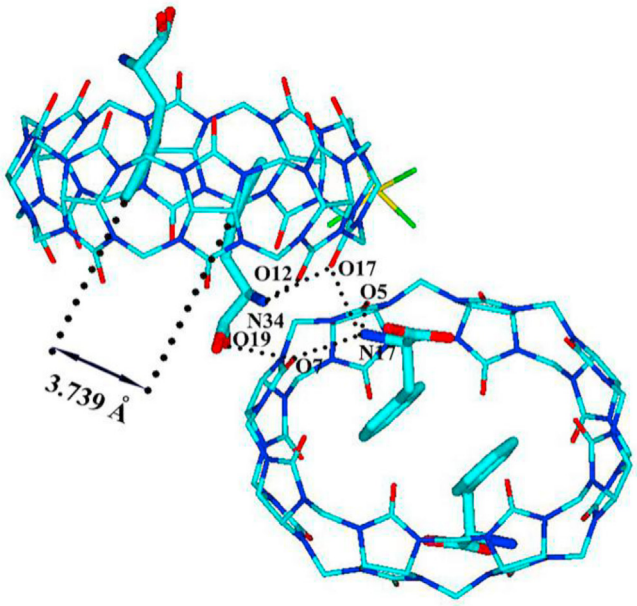

Fig. 9. The molecular structure of the homo-ternary complex, ***L*-Phe** 2@Q[8].

replaced by the *L*-Trp molecule in the Q[8] cavity, consistent with the observations for the Q[8]-AC- *L*-Phe system.

Similarly, the crystallization of Q[8]-L-Phe was conducted in an aqueous HCl solution (6.0 M) by introducing $[CdCl_4]^{2-}$; the crystal structure is shown in Fig. 9. The two *L*-Phe guest molecules with π···π interactions (the distance between two aromatic rings is 3.739 Å) are located in the Q[8] cavity forming a 1:2 stoichiometry host-guest inclusion complex, and the presence of the hydrogen bonds of *N*–H···O between *L*-Phe and carbonyl oxygen of Q[8] is beneficial to the stability of the system. Multiple hydrogen-bonding interactions between Q[8]-dimers, which involve *O*–H···O and *N*–H···O between *L*-Phe and a portal carbonyl group (O19···O7 = 2.508 Å, N17···O5 = 2.809 Å, N17···O7 = 2.963 Å, N17···O17 = 2.852 Å, N34···O12 = 2.911 Å, and N34···O17 = 2.968 Å) can be observed (see Fig. 9).

3. Experimental section

3.1. Materials

The cucurbituril Q[8] was synthesized according to a procedure developed previously in our laboratory. Acridine and the amino acids were purchased from Aladdin (Shanghai, China). All other reagents were of analytical reagent quality and were used without any further purification. Doubly-distilled water was employed throughout.

3.2. Measurement of absorption, mass and fluorescence spectra

UV–visible spectra were recorded on an Agilent 8453 spectrophotometer (Agilent Technologies, Santa Clara, CA, USA) using solutions in 1 cm quartz cells. MALDI-TOF mass spectra were obtained using a Bruker BIFLEX III ultra-high resolution Fourier transform ion cyclotron resonance (FT-ICR) mass spectrometer using α-cyano-4-hydroxycinnamic acid as the matrix.

Fluorescence emission spectra were collated using a VARIAN Cary Eclipse spectrofluorometer (Varian, Inc., Palo Alto, CA, USA). Stock solutions of Q[8] (1.00×10^{-4} mol L^{-1}), acridine hydrochloride (**AC**, 1.00×10^{-3} mol L^{-1}) and *L*-amino acids

(2.00×10^{-2} mol L^{-1}) were prepared using doubly-distilled water. The test solutions were prepared by diluting the stock solutions to the required concentrations.

Aqueous solutions of **AC** (2.0×10^{-5} mol L^{-1}) were prepared by diluting the stock solutions. For the absorption and fluorescence spectra, increasing concentrations (0–3.0×10^{-5} mol L^{-1}) of Q[8] solution were added to the free **AC** and the pH was adjusted to 4.0 via the addition of concentrated hydrochloric acid. Aqueous solutions of the AC/Q[8] complex (**AC**: 2.0×10^{-5} mol L^{-1}) were prepared for characterization by fluorescence emission spectroscopy. To obtain fluorescence spectra, known concentrations of amino acids were added to the AC/Q[8] complex. Fluorescence spectra were obtained by excitation at 346 nm with 5 nm emission and excitation bandwidths, and the emission intensity was monitored at 478 nm at ambient temperature. The maximum emission wavelength was λem = 478 nm for the **A**C/Q[8] complex. To obtain titration fluorescence spectra, *L*-Phe (1.5, 3.0, 4.5·····45.0 μl, 2.00×10^{-2} mol L^{-1}) was added to the Q[8]-AC (3 mL, 2.00×10^{-5} mol L^{-1}) complex in quartz cells.

3.3. ^{1}H NMR measurements

The ^{1}H NMR spectra were recorded at 25 °C on a JEOL JNM-ECZ400s spectrometer. D_2O, adjusted to pH 4 via addition of DCl, was used as a field-frequency lock. The observed chemical shifts are reported in parts per million (ppm) relative to that of the internal tetramethylsilane (TMS) standard (0.0 ppm).

3.4. Synthesis of guest AC

Acridine (358 mg, 0.002 mol) was dissolved in concentrated HCl (10 mL), and the solution was then stirred under an inert nitrogen atmosphere, and heated to 80 °C and refluxed for a further 6 h. The resulting solution was spin-dried and the yellow precipitate was washed with diethyl ether and dried *in vacuo* to afford **AC** (366 mg, 85%). ^{1}H NMR (D_2O, 400 MHz) δ 9.74 (s, 1H), 8.37 (d, J = 8.6 Hz, 2H), 8.22–8.15 (m, 4H), 7.83 (d, J = 8.3, 6.0 Hz, 2H). Anal. Calcd. for $C_{13}H_{10}NCl$: C, 72.40; H, 4.67; N, 6.49; found C, 72.07; H, 4.81; N, 6.52.

3.5. Crystallization and structure determination

Synthesis of the inclusion complex Q[8]-**AC (CCDC 1962675)** Q[8] (7.54 mg, 0.005 mmol), **AC** (10.78 mg, 0.050 mmol) and $CdCl_2 \cdot 4H_2O$ (11.8 mg, 0.051 mmol) were dissolved in HCl (4 mL, 6 mol/L). The mixture was heated until complete dissolution. Slow evaporation of the volatiles from the solution over a period of about two weeks provided buff colored crystals.

Synthesis of the inclusion complex Q[8]-***L*-Phe (CCDC 1962676)** Q[8] (7.54 mg, 0.005 mmol), *L*-Phe (8.26 mg, 0.050 mmol) and $CdCl_2 \cdot 4H_2O$ (11.8 mg, 0.051 mmol) were dissolved in HCl (4 mL, 6 mol/L). The mixture was heated until complete dissolution. Slow evaporation of the volatiles from the solution over a period of about two weeks provided colorless crystals.

All structure determination details are presented in Table S3, ESI.

Diffraction data for the complexes were collected at 298 K with Bruker D8 VENTURE diffractometer and Bruker SMART Apex-II CCD diffractometer.

4. Conclusions

In summary, a new "on-off-on" fluorescent chemosensor based on cucuribit [8]uril (Q[8]) and acridine hydrochloride (AC) has been successfully constructed and utilized for the recognition of different amino acids. In aqueous solution, AC was encapsulated within the Q[8] cavity to form a 1:2 host-guest inclusion complex, which was verified in the solid-state by a single-crystal X-ray structural determination. Free AC is known to be strongly fluorescent, however this strong fluorescence was extinguished in the Q[]-AC inclusion complex. This non-fluorescent Q[8]-AC complex served as a fluorescence "off-on" probe capable of recognizing *L*-Phe or *L*-Trp, owing to the competitive interaction between *L*-Phe or L-Trp; the included AC molecule is replaced by the *L*-Phe or *L*-Trp molecule in the Q[8] cavity. This fluorescent chemosensor also possessed pH-responsiveness, where the addition of basic L-amino acids (L-Arg, L-His or L-Lys) caused blue shift fluorescence changes for the Q[8]-AC complex. This work led to a fluorescence method for the detection of five amino acids in a single system. The method presented in this investigation represents a promising potential practical application for the detection of amino acids.

CRediT authorship contribution statement

Weitao Xu: participated in the design of this study, Formal analysis, Conception, design of the study, acquisition of data, Formal analysis, and interpretation of data, drafting the article or revising it critically for intellectual content, All authors read and approved the final manuscript. **Huaming Feng:** carried out the study and collected important background information, Conception, design of the study, acquisition of data, Formal analysis, drafting the article or revising it critically for intellectual content, All authors read and approved the final manuscript. **Weiwei Zhao:** carried out the study and collected important background information, Conception, design of the study, acquisition of data, Formal analysis, drafting the article or revising it critically for intellectual content, All authors read and approved the final manuscript. **Chunhua Huang:** drafted the manuscript, Conception, design of the study, acquisition of data, Formal analysis, drafting the article or revising it critically for intellectual content, All authors read and approved the final manuscript. **Carl Redshaw:** carried out the concepts, design, definition of intellectual content, literature search, data acquisition, Formal analysis, manuscript preparation, design of the study, acquisition of data, Formal analysis, and interpretation of data, drafting the article or revising it critically for intellectual content, All authors read and approved the final manuscript. **Zhu Tao:** provided assistance for data acquisition, Formal analysis, statistical . **Xin Xiao:** carried out literature search, data acquisition, manuscript editing, Conception, design of the study, acquisition of data, Formal analysis, drafting the article or revising it critically for intellectual content, All authors read and approved the final manuscript.

Declaration of competing interest

The authors declare that they have no known competing financial interests or personal relationships that could have appeared to influence the work reported in this paper.

Acknowledgements

We thank the National Natural Science Foundation of China (NSFC no 21861011), the Major Program for Creative Research Groups of Guizhou Provincial Education Department (2017–028) and the Innovation Program for High-level Talents of Guizhou Province (No. 2016–5657) are gratefully acknowledged for financial support. CR thanks the EPSRC for an Overseas Travel Grant (EP/S025537/1).

Appendix A. Supplementary data

Supplementary data to this article can be found online at https://doi.org/10.1016/j.aca.2020.09.028.

References

[1] S. Berliner, Adv. Nurse Pract. 14 (2006) 47–48.
[2] V.I. Chalova, I.B. Zabala-Diaz, C.L. Woodward, S.C. Ricke, World J. Microbiol. Biotechnol. 24 (2007) 353–359.
[3] S. Kado, H. Otani, Y. Nakahara, K. Kimura, Chem. Commun. 49 (2013) 886–888.
[4] V.K. Gupta, A.K. Jain, G. Maheshwari, H. Lang, Z. Ishtaiwi, Sensor. Actuator. B Chem. 117 (2006) 99–106.
[5] R.N. Goyal, V.K. Gupta, N. Bachheti, Anal. Chim. Acta 597 (2007) 82–89.
[6] R.N. Goyal, V.K. Gupta, S. Chatterjee, Biosens. Bioelectron. 24 (2009) 1649–1654.
[7] R.N. Goyal, V.K. Gupta, Chatterjee, Electrochim. Acta. 53 (2008) 5354–5360.
[8] F. Schneider, Angew Chem. Int. Ed. Engl. 17 (1978) 583–592.
[9] J. Maeda, M. Higashiyama, A. Imaizumi, T. Nakayama, H. Yamamoto, T. Daimon, M. Yamakado, F. Imamura, K. Kodama, BMC Canc. 10 (2010) 690.
[10] Y. Miyagi, M. Higashiyama, A. Gochi, M. Akaike, T. Ishikawa, T. Miura, N. Saruki, E. Bando, H. Kimura, F. Imamura, M. Moriyama, I. Ikeda, A. Chiba, F. Oshita, A. Imaizumi, H. Yamamoto, H. Miyano, K. Horimoto, O. Tochikubo, T. Mitsushima, M. Yamakado, N. Okamoto, PloS One 6 (2011), e24143.
[11] H.J. Kim, S.H. Jang, J.S. Ryu, J.E. Lee, Y.C. Kim, M.K. Lee, T.W. Jang, S.Y. Lee, H. Nakamura, N. Nishikata, M. Mori, Y. Noguchi, H. Miyano, K.Y. Lee, Lung Canc. 90 (2015) 522–527.
[12] X. Bi, C.J. Henry, Nutr. Diabetes 7 (2017), e249.
[13] E. Simin´ska, M. Koba, Amino Acids 48 (2016) 1339–13452.
[14] H. Yoshida, Y. Nakano, K. Koiso, H. Nohta, J. Ishida, M. Yamaguchi, Anal. Sci. 17 (2001) 107–112.
[15] D. Wellner, A. Meister, Annu. Rev. Biochem. 50 (1981) 911–968.
[16] P. Felig, Annu. Rev. Biochem. 44 (1975) 933–955.
[17] C. Hirayama, K. Suyama, Y. Horie, K. Tanimoto, S. Kato, Biochem. Med. Metab. Biol. 38 (1987) 127–133.
[18] Y.M. Fu, H. Zhang, M.J. Ding, Y.Q. Li, X. Fu, Z.X. Yu, G.G. Meadows, J. Cell. Physiol. 209 (2006) 522–534.
[19] A.K. Saini, M. Saraf, P. Kumari, S.M. Mobin, New J. Chem. 42 (2018) 3509–3518.
[20] S. Russo, I.P. Kema, R.M. Fokkema, J.C. Boon, P.H.B. Willemse, E.G.E. de Vries, J.A. Den Boer, J. Korf, Psychosom. Med. 65 (2003) 665–671.
[21] R.S. Staden, R.M. Nejem, J.F. Staden, H.Y. Aboul-Enein, Biosens. Bioelectron. 35 (2012) 439–442.
[22] M. Ebata, Y. Takahashi, H. Otsuka, J. Chromatogr., A 25 (1966) 1–10.
[23] V.K. Gupta, A.K. Singh, M.A. Khayat, B. Gupta, Anal. Chim. Acta 590 (2007) 81–90.
[24] R.J. DeLange, D.M. Fambrough, E.L. Smith, J. Bonner, J. Biol. Chem. 243 (1968) 5906–5913.
[25] P. Das, A.K. Mandal, R.G. Upendar, M. Baidya, S.K. Ghosh, A. Das, Org. Biomol. Chem. 11 (2013) 6604–6614.
[26] H.S. Jung, J.H. Han, T. Pradhan, S. Kim, S.W. Lee, J.L. Sesslerc, T.W. Kim, C. Kang, J.S. Kim, Biomaterials 3 (2012) 945–953.
[27] T. Matsumoto, Y. Urano, T. Shoda, H. Kojima, T. Nagano, Org. Lett. 9 (2007) 3375–3377.
[28] R.N. Dsouza, U. Pischel, W.M. Nau, Chem. Rev. 111 (2011) 7941–7980.
[29] L. You, D. Zha, E.V. Anslyn, Chem. Rev. 115 (2015) 7840–7892.
[30] W.L. Mock, N.Y. Shih, J. Am. Chem. Soc. 110 (1988) 4706–4710.
[31] J.W. Lee, S. Samal, N. Selvapalam, H.J. Kim, K. Kim, Acc. Chem. Res. 36 (2003) 621–630.
[32] R.H. Gao, L.X. Chen, K. Chen, Z. Tao, X. Xiao, Coord. Chem. Rev. 348 (2017) 1–24.
[33] D. Bai, X. Wang, Z.Z. Gao, S.C. Qiu, Z. Tao, J.X. Zhang, X. Xiao, Chin. J. Org. Chem. 37 (2017) 2022–2027.
[34] J.J. Lian, P. Liu, X.C. Li, L.N. Gao, X.L. Luo, X. Zhang, Z.Q. Shi, Q.Y. Liu, Appl. Organomet. Chem. (2019), e4884.
[35] Y. Gao, C. Jin, X. Li, K. Wu, L. Gao, X. Lyu, X. Zhang, X. Zhang, X. Luo, Q. Liu, Colloid Surface A 568 (2019) 248–258.
[36] J. Lagona, P. Mukhopadhyay, S. Chakrabarti, L. Isaacs, Angew. Chem. Int. Ed. 44 (2005) 4844–4870.
[37] S.M. Liu, C. Ruspic, P. Mukhopadhyay, S. Chakrabarti, P.Y. Zavalij, L. Isaacs, J. Am. Chem. Soc. 127 (2005) 15959–15967.
[38] X.Yu Deng, K. Chen, M.D. Chen, L.B. Lü, Z. Tao, Eur. J. Inorg. Chem. 9 (2019) 1212–1219.
[39] X.Y. Deng, W.T. Xu, M. Liu, M.X. Yang, Q.J. Zhu, B. Lü, Z. Tao, Supramol. Chem. 31 (2019) 616–624.
[40] L.A. Logsdon, A.R. Urbach, J. Am. Chem. Soc. 135 (2013) 11414–11416.
[41] M.V. Rekharsky, H. Yamamura, Y.H. Ko, N. Selvapalam, K. Kim, Y. Inoue, Chem. Commun. 19 (2008) 2236–2238.
[42] P.H. Shan, S.C. Tu, R.L. Lin, Z. Tao, J.X. Liu, X. Xiao, CrystEngComm 19 (2017) 2168–2171.
[43] O. Danylyuk, CrystEngComm 19 (2017) 3892–3897.
[44] J. Lee, L. Perez, Y. Liu, H. Wang, Richard J. Hooley, W.W. Zhong, Anal. Chem. 90 (2018) 1881–1888.
[45] L.C. Smith, D.G. Leach, B.E. Blaylock, O.A. Ali, A.R. Urbach, J. Am. Chem. Soc. 137 (2015) 3663–3669.
[46] P.H. Shan, J. Zhao, X.Y. Deng, R.L. Lin, B. Bian, Z. Tao, X. Xiao, J.X. Liu, Anal. Chim. Acta 1104 (2020) 164–171.
[47] M.X. Yang, M. Liu, M. Yang, Q. Wang, X. Zeng, Z. Tao, X. Xiao, Y. Huang, Inorg. Chem. Commun. 108 (2019) 107514–107522.
[48] P. Rajgariah, A.R. Urbach, J. Inclusion Phenom. Macrocycl. Chem. (2008) 251–254.
[49] M del Pozo, P. Hernandez, L. Hernandez, C. Quintana, J. Mater. Chem. 21 (2011) 13657–13663.
[50] Q.H. Bai, S.W. Zhang, H.R. Chen, T. Sun, C. Redshaw, J.X. Zhang, X.L. Ni, G. Wei, Z. Tao, Chemistry 2 (2017) 2569–2573.
[51] X.K. Yu, W.T. Liang, Q.F. Huang, W.H. Wu, Jason J. Chruma, C. Yang, Chem. Commun. 55 (2019) 3156–3159.
[52] P. Wang, Y. Yao, M. Xue, Chem. Commun. 50 (2014) 5064–5067.